Coherent superposition of laser-driven soft-X-ray harmonics from successive sources

J. SERES[1,2], V. S. YAKOVLEV[3], E. SERES[1,2], CH. STRELI[4], P. WOBRAUSCHEK[4], CH. SPIELMANN[2] AND F. KRAUSZ[3,5]*

[1]Institut für Photonik, Technische Universität Wien, A-1040 Wien, Austria
[2]Physikalisches Institut EP1, Universität Würzburg, D-97074 Würzburg, Germany
[3]Department für Physik, Ludwig-Maximilians-Universität München, D-85748 Garching, Germany
[4]Atominstitut der Österreichischen Universtitäten, Technische Universität Wien, A-1020 Wien, Austria
[5]Max-Planck-Institut für Quantenoptik, D-85748 Garching, Germany
*e-mail: krausz@lmu.de

Published online: 11 November 2007; doi:10.1038/nphys775

High-order harmonic generation from atoms ionized by femtosecond laser pulses has been a promising approach for the development of coherent short-wavelength sources. However, the realization of a powerful harmonic X-ray source has been hampered by a phase velocity mismatch between the driving wave and its harmonics, limiting their coherent build-up to a short propagation length and thereby compromising the efficiency of a single source. Here, we report coherent superposition of laser-driven soft-X-ray (SXR) harmonics, at wavelengths of 2–5 nm, generated in two successive sources by one and the same laser pulse. Observation of constructive and destructive interference suggests the feasibility of quasi-phase-matched SXR harmonic generation by a focused laser beam in a gas medium of modulated density. Our proof-of-concept study opens the prospect of enhancing the photon flux of SXR harmonic sources to levels enabling researchers to tackle a range of applications in physical as well as life sciences.

The quest for powerful laboratory sources of coherent soft-X-ray (SXR) light has been ongoing since the discovery of the laser. So far, high-order harmonic generation from atoms ionized by ultrashort laser pulses[1,2] constitutes the only technique providing coherent short-wavelength radiation at any photon energy up to the kiloelectronvolt regime[3–11]. Laser-driven high-harmonic sources (henceforth briefly referred to as harmonic sources) up to photon energies of 100 eV are now in widespread use[12] and have played a key role in pushing the frontiers of nonlinear optics into the extreme-ultraviolet region[13–17] and ultrafast science into the attosecond domain[18–23]. Above 100 eV, rapidly decreasing efficiency prevented harmonic sources from becoming useful for applications. The low harmonic conversion efficiency implies that most of the incident laser photons are transmitted through the harmonic source, offering the possibility of being reused for creating harmonics in successive sources and—by exploiting their coherence—adding them to increase the overall harmonic flux. Here, we demonstrate the feasibility of this approach.

Efficient generation of high-order harmonics of intense laser light relies on a large number of ionizing atoms emitting high-frequency radiation with proper phase that allows coherent build-up of light on propagation through the generation medium. Free electrons, unavoidable concomitants of the generation process, tend to severely limit the propagation length over which phase-matching can be achieved (henceforth briefly referred to as the coherence length). Femtosecond laser pulses have permitted the generation of harmonics in the extreme-ultraviolet regime (10–100 eV) at sufficiently low levels of ionization, so that the coherence length could be extended beyond the absorption length[4,5], leading to the production of microjoule-energy coherent extreme-ultraviolet pulses[6,7].

Generation of SXR harmonics (>100 eV) is favoured by lowered absorption but suffers from increased free-electron density implied by the higher laser intensities required. Hence, the efficiency of SXR harmonic sources is limited by dephasing of the atomic dipole oscillators driven at different positions in the generation medium[24]. The SXR harmonic yield has recently been improved by implementing quasi-phase-matching (QPM) in a gas-filled hollow-core fibre with a modulated inner diameter[8] or counter-propagating laser pulses[25,26]. At higher photon energies, subcycle modification of few-cycle driving fields has been identified as being beneficial for enhancing phase-matching[27] (referred to as non-adiabatic self-phase-matching), which allowed extension of harmonic generation beyond the kiloelectronvolt frontier[10,11]. Unfortunately the fluxes demonstrated so far are still insufficient for most applications.

Here, we provide the first experimental evidence of the feasibility of enhancing the efficiency of SXR harmonic generation by coherent superposition of harmonics generated in successive sources traversed by the same pump laser beam (Fig. 1). SXR harmonic emission from a single source is maximized by using few-cycle driver pulses, which maximize both the single-atom emission intensity and the coherence length for SXR harmonics[24], and is limited by dephasing. The phase of the atomic dipole

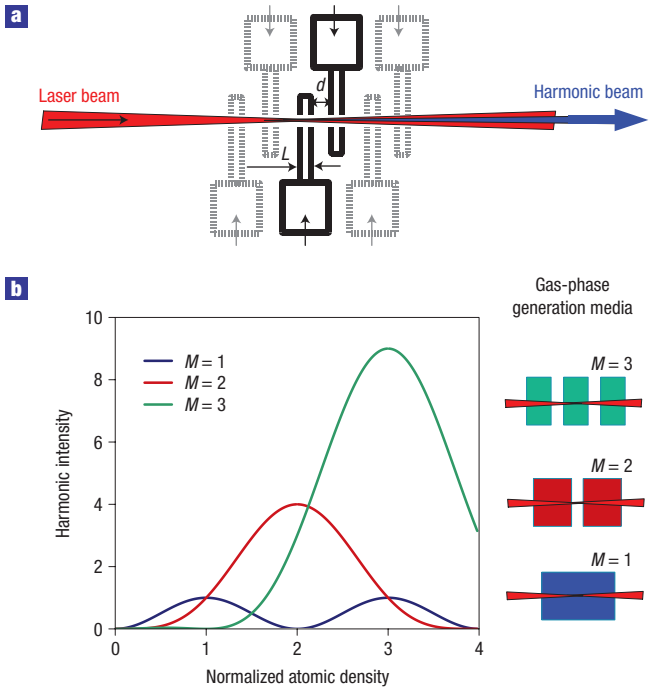

Figure 1 High-order harmonic generation from successive sources. **a**, Schematic diagram of a sequence of harmonic sources formed by gas-phase generation media enclosed in thin tubes described in the main text. The sources are arranged along the optical axis of a (gently) focused laser beam and pumped by the same laser pulse. In the present proof-of-concept study we have used only two sources (shown in black); further sources can be added for scaling the SXR harmonic yield in future experiments (shown in grey). **b**, Increasing the density of atomic dipole emitters tends to increase the coherent harmonic yield. However, increasing density causes the dipole oscillators to increasingly dephase along the laser propagation direction. In a single source, this leads to saturation of the harmonic yield at a normalized atomic density of $N_a/N_{a,q}=1$ according to equation (3) (blue curve). Splitting the generation medium into two or three equal sections and moving them apart so that the phase of the atomic dipole oscillations gets shifted by π in the focused laser beam allows the atomic density to be increased by a factor of 2 and 3, respectively, leading to saturation at a factor of 4 and 9 higher harmonic intensities (red and green curves), respectively.

oscillators is restored in the second source by diffraction-induced changes in the laser phase and amplitude on propagation between the two sources. The approach embodies the basic concept of QPM and is superior to previous implementations of QPM in several respects.

First, it is scalable to higher laser intensities and, consequently, to higher photon energies without compromising the lifetime of the system components (in contrast to the degradation of the hollow-core waveguide in previous implementations of QPM[8,28]). Second, rephasing occurs during loss-free propagation, allowing the highest possible conversion efficiency any QPM scheme can offer to be reached. Third, and most importantly, the new scheme allows emission yields from the individual sources and constructive interference between them to be maximized by their independent optimization (for example, in terms of particle density) and appropriate positioning of the sources in the focused laser beam. Implemented with few-cycle driver pulses, this approach therefore opens the prospect of matching the phase of kiloelectronvolt-scale harmonic emission from a large number of atoms, to create coherent kiloelectronvolt radiation that is powerful enough to enable high-resolution spectroscopy in the time and frequency domains.

THEORETICAL BACKGROUND

To shed light on the basic operational principle of harmonic generation from a series of independent sources, we resort to the simplest possible model of the phenomenon. Here, the single-atom emission amplitude is assumed to be the same for all atoms and the phase mismatch $z\Delta k$ is assumed to grow linearly with the propagation distance z; the intensity I_q of the qth harmonic of the laser frequency ω_L generated in a source of length L is given by

$$I_q \propto N_a^2 \frac{\sin^2\left(\frac{L\Delta k}{2}\right)}{(\Delta k)^2}, \qquad (1)$$

where N_a is the number of atomic dipole radiators created by the driving pulse. If dephasing is dominated by free electrons, as is usually the case for high-order harmonics, the phase mismatch $L\Delta k$ scales with the density N_e of free electrons, $\Delta k \propto N_e \propto N_a$ (see, for example, refs 28,29), so that

$$I_q \propto \sin^2\left(\frac{L\Delta k}{2}\right) = \sin^2\left(\frac{\pi N_a}{2N_{a,q}}\right). \qquad (2)$$

Here $N_{a,q}$ is the largest density, for which the qth harmonic monotonically grows over the propagation distance L. A further increase of N_a by increasing the gas pressure will decrease the harmonic yield because the phase mismatch will cause a destructive interference of harmonic photons generated in the first half and the second half of the source.

The onset of destructive interference can be shifted to higher atomic densities, and hence enhanced harmonic yields, by subdividing the overall interaction length L into M sections of thickness L/M and moving them apart such that diffraction-induced changes in the laser phase and amplitude between two adjacent sections can shift the phase of the atomic dipole oscillations by π (at the input of the next section with respect to the exit of the previous one) at a given frequency, say $\omega_q = q\omega_L$. Then the yield of the qth harmonic at ω_q takes the form

$$I_q \propto \frac{1-(-1)^M\cos\left(\pi\frac{N_a}{N_{a,q}}\right)}{1+\cos\left(\frac{\pi}{M}\frac{N_a}{N_{a,q}}\right)}\sin^2\left(\frac{\pi}{2M}\frac{N_a}{N_{a,q}}\right). \qquad (3)$$

This modification allows us to increase the atomic density by a factor of M, resulting in a harmonic yield enhanced by a factor of M^2, as illustrated for two and three sections in Fig. 1b.

EXPERIMENTAL SET-UP

In our experiments 750 nm, 2 mJ, 15 fs pulses at a repetition rate of 1 kHz (ref. 30) are spectrally broadened in a filament[31] formed in argon (0.6 bar) and temporally compressed to a ~1 mJ, ~5 fs pulse accompanied by a 0.5 mJ pedestal distributed over an interval of ~15 fs. The few-cycle near-infrared pulse is focused into the interaction region to a $1/e^2$ diameter of $2w_0 = 93 \pm 5\,\mu$m, corresponding to a confocal parameter of $b = 2\pi w_0^2/\lambda_L \approx 18$ mm. This results in an effective temporal peak intensity (averaged over $A_{eff} = \pi w_0^2$) of $\approx 3 \times 10^{15}$ W cm^{-2} and implies an effective cutoff energy in the single-atom radiation spectrum of about 0.6 keV.

The interaction between the laser beam and the helium gas takes place within a pair of nickel tubes with their axes aligned perpendicularly to the laser beam axis. The inner diameter of

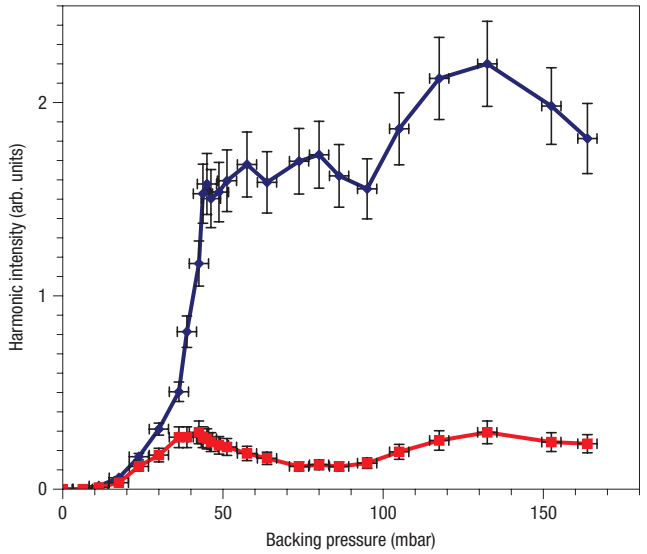

Figure 2 Scaling of SXR harmonic yield with particle density. Harmonic photon yield within a 32 eV band at 330 eV (blue curve) and at 375 eV (red curve) from a single (merged) source versus backing pressure. The vertical error bars represent standard deviations of photon counts; the horizontal error bars represent the 10 mbar uncertainty in the gas pressure that stems from the hysteresis of the piezo-based pressure meter.

the tubes (0.8 mm) was squeezed to $L \approx 0.2$ mm. The laser drills holes in the thin (0.1 mm) tube walls, the diameters of which are precisely matched to that of the beam, minimizing gas load to the surrounding vacuum ($p_{\mathrm{chamber}} < 0.5$ mbar). As gas is effusing through the holes, the effective interaction length in each source is estimated as $L_{\mathrm{eff}} \approx 0.4$ mm. The tubes are fed continuously with helium gas and mounted on three-axis translation stages.

The harmonic radiation emerging collinearly with the laser beam hits a cooled (77 K) lithium-drifted silicon crystal detector 80 cm downstream of the sources. A set of thin metal filters (see caption of Fig. 4) and pinholes block low-order harmonics and the laser beam and attenuate the SXR photon flux to a level of less than 0.1 photon per laser pulse in front of the single-photon-counting Si(Li) X-ray detector. Photon counts are collected in 16 eV bins by a multichannel analyser. The resolution of this energy-dispersive detection system at the carbon K_α line is ≈70 eV (full-width at half-maximum: FWHM). We have recorded a series of harmonic spectra at photon energies $\hbar\omega_{\mathrm{X}} > 200$ eV as a function of the atomic gas density and the distance d between the two sources (d was measured between the centres of the sources, therefore $d \geq 0.4$ mm).

HARMONIC EMISSION FROM A SINGLE SOURCE

First, we optimized the SXR harmonic yield from a single source by merging the two sources into one with an effective length of $L_{\mathrm{eff}} \approx 0.8$ mm. Maximum SXR yield was found to be achievable for the single (merged) source ($M = 1$) being positioned approximately 1 mm downstream from the waist of the laser beam, in accordance with previous observations[32]. Figure 2 shows the harmonic yield at photon energies of 330 eV and 375 eV, as measured within a 32 eV band as a function of the backing pressure, p_{b}. The SXR yield increases near-quadratically with particle density up to $p_{\mathrm{b}} \approx 40$ mbar, followed by saturation at higher densities, indicating the onset of destructive interference. From gas flow simulations, we infer a particle density in the interaction region that is 2–3 times smaller than the backing density, with the uncertainty originating from that of the diameter of the laser-drilled holes. This implies that the maximum yield from the single source of $L_{\mathrm{eff}} \approx 0.8$ mm is achieved at target pressures in excess of 10 mbar.

In striking contrast, plasma-dispersion-induced dephasing is predicted to limit the coherence length to less than the effective source length at target pressures below 1 mbar in the 300–400 eV spectral range. In our experiment, phase-matching is observed up to >10-times higher pressures, resulting in a >100-fold increase in SXR harmonic yield. The enhanced phase-matching of SXR harmonics observed in our experiments relates to the fact that the phase of high-order harmonics emitted by individual atoms is sensitive to even minuscule changes of the driving-field oscillations during propagation. This sensitivity originates from the large phase shift the electron wavepacket accumulates during its long excursion between the ionization and recollision moments in the strongly driven atom. As a consequence, a decrease of the driving-field amplitude (due to beam divergence behind the focus) as well as an increase of its instantaneous frequency[33] (due to ionization) tends to compensate for the phase mismatch that originates from the plasma dispersion and the Gouy phase shift. The fact that our source delivers a substantially enhanced SXR yield when positioned behind the focus suggests that the former (amplitude) effect might provide the dominant contribution to enhanced SXR harmonic phase-matching under our experimental conditions. This effect is also found to play an important role in restoring the harmonic phase between subsequent sources and will be elaborated on in the discussion.

HARMONIC EMISSION FROM SUCCESSIVE SOURCES

Figure 2 shows that the SXR harmonic yield from a single source levels off at backing pressures above 40 mbar because the atomic dipoles in the second half of the source start radiating out of phase with those in the first half of the source. To verify this conjecture, we compared the SXR harmonic spectra recorded at $p_{\mathrm{b}} \approx 120$ mbar with the second half of the merged source switched off and on, see the green and purple curves in Fig. 3a, respectively. With the second source switched on, the harmonic yield is enhanced at photon energies below ~240 eV. More importantly, the signal is reduced, to an increasing extent with increasing photon energies above 240 eV, providing clear evidence for destructive interference between the coherent SXR radiation originating from the first and second sources.

Separation of the two sources may offer a route to restoring the proper phase relationship between the SXR waves emerging from them and give way for further enhancement of the yield according to the above considerations (see Fig. 1 and related discussion). Moving the second source to an optimum distance ($d \approx 1.7$ mm) from the first one turns destructive interference in the region around 300 eV into constructive interference, resulting in a 10-fold increase of coherent SXR harmonics, as revealed by the dashed line in Fig. 3a showing the ratio of the harmonic yield from the separated sources to that emerging from the merged sources. Control of coherent superposition of laser-induced soft-X-ray harmonics from successive sources is conclusively demonstrated by these results.

Figure 3b provides further compelling evidence for interference between harmonic signals emerging from the successive sources. It shows the harmonic photon yield collected in two bins around $\hbar\omega_{\mathrm{X}} \approx 390$ eV as a function of the gas density with the two sources merged ($d = 0.4$ mm) and separated by $d = 1.7$ mm, yielding maximum output in this energy band. The dependence of the harmonic yield on the gas pressure was fitted using equation (3)

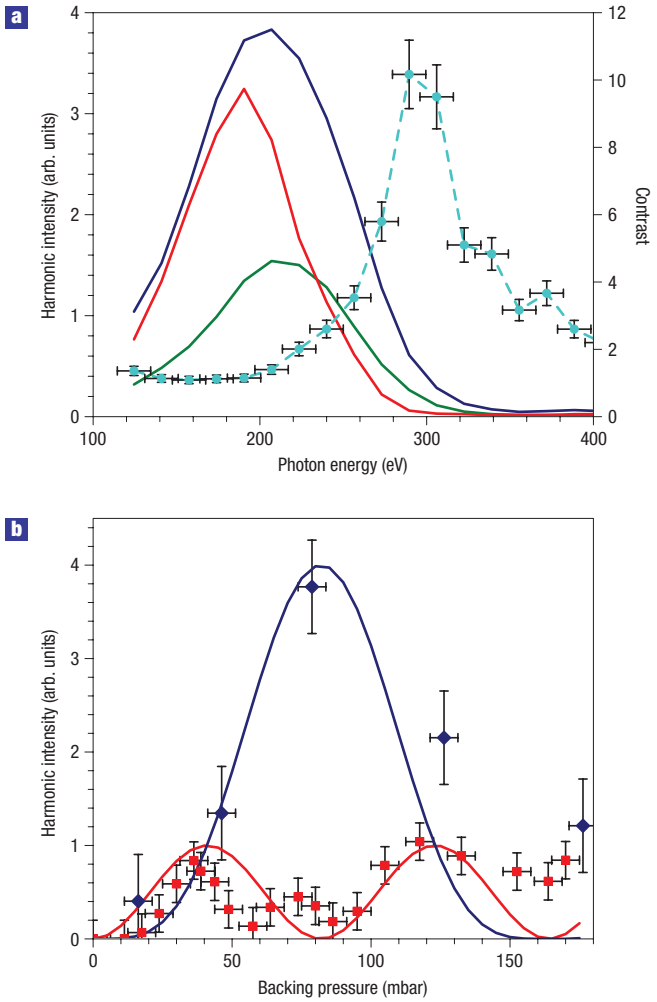

Figure 3 Destructive and constructive interference of SXR harmonics from successive sources. a, Harmonic spectra from a single 0.4-mm-thick source placed approximately 1 mm downstream from the beam waist of the pump laser beam (green curve) and from two identical 0.4-mm-thick successive sources with the second source pushed to close proximity of the first one (red curve) and removed from the first source so that their centres were separated by $d \approx 1.7$ mm (blue curve). The backing pressure for both sources was 120 mbar. The dashed line shows the ratio of the harmonic yields from the successive sources placed at optimum separation (blue curve) and merged (red curve) on the scale shown on the right vertical axis (the vertical error bars are standard deviations and the horizontal error bars correspond to the channel width of the spectrograph). All spectra were recorded with the filter set described in the caption of Fig. 4. **b**, Squares: harmonic yield measured with the two sources merged (separation between their centres: $d = 0.4$ mm) to form a single continuous gas medium with an effective length of $L_{\mathrm{eff}} \approx 0.8$ mm. Diamonds: harmonic yield obtained for the two sources separated by $d = 1.7$ mm. The lines show fits to the measured data by using the prediction of a simple adiabatic model of the build-up of a coherent harmonic signal, as given by equation (3). The error bars represent standard deviations.

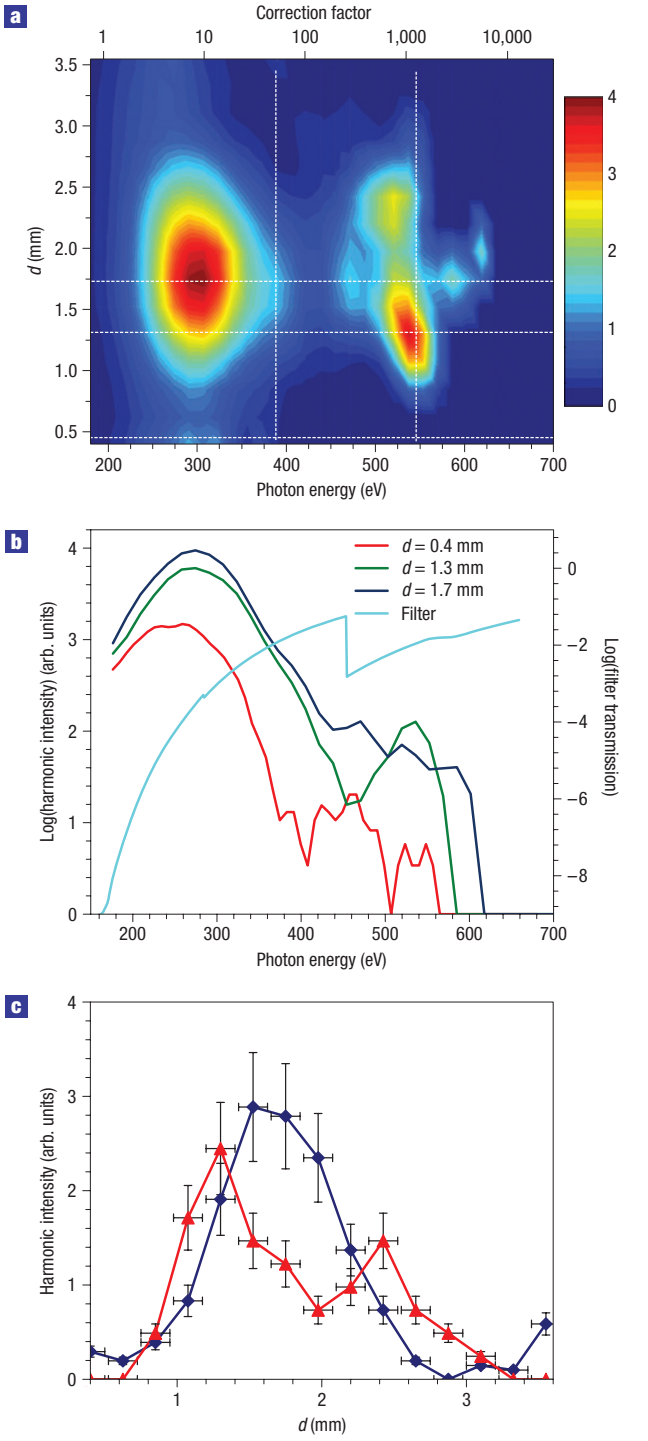

Figure 4 SXR harmonics generated in successive sources. a, Harmonic yield versus photon energy and source separation, in a false-colour representation. The rapid roll-off of the yield with photon energy has been corrected by the exponential factor shown above the panel. This correction allowed the harmonic yield to be plotted on a linear scale and thereby the pronounced variation of the harmonic intensity with source distance can be seen. **b**, Harmonic spectra recorded at three different source distances. Transmittivity of the set of filters placed in front of the Si(Li) detector and materials incorporated in the detector in front of the p–n junction, including 300 nm aluminium, 200 nm titanium, 100 nm carbon and 100 nm silicon. **c**, Variation of the harmonic yield with source distance at two selected photon energies, $\hbar\omega_X = 390$ eV (diamonds) and $\hbar\omega_X = 535$ eV (triangles). The error bars are standard deviations.

with $M = 1$ and $M = 2$, respectively. The best agreement is attained with a backing pressure (resulting in $N_{a,q}$) of $p_q = 43$ mbar. Our highly simplified model summarized in equations (1)–(3) accounts remarkably well for the observed behaviour. Most importantly, at approximately twice the 'phase-matching pressure', $p = 2p_q$, the harmonic signal from the sources merged ($d = 0.4$ mm) drops

close to zero, whereas it reaches a maximum from the separated sources ($d = 1.7$ mm) that exceeds by a factor of four the harmonic yield obtained from the merged sources at $p = p_q$. This agreement with our simple considerations discussed above indicates that SXR harmonic waves originating from two successive sources can be added to yield a wave delivering four times as many X-ray photons as the individual waves, or cancel each other to yield near-zero output.

Figure 4a shows harmonic spectra measured at $p = 80$ mbar, which resulted in the strongest destructive interference (minimum yield) near 400 eV for the sources merged. For the best assessment of the variation of the harmonic signal with d, we have chosen to correct for the rapid roll-off of the harmonic intensity with an exponential factor and plotted the corrected harmonic intensity on a linear scale. In the range of $200\,\text{eV} < \hbar\omega_X < 400\,\text{eV}$, the harmonic yield peaks at $d_{\text{max,200–400}} \approx 1.7$ mm with a FWHM of the signal distribution of $d_{\text{FWHM,200-400}} \approx 1.0$ mm. The maximum photon yield within a 10% band at $\hbar\omega_X = 300$ eV is estimated as 10^5–10^6 photons s^{-1}. The dependence of the harmonic yield on source distance is similar in this entire octave-spanning spectral range. At higher photon energies we observe a different behaviour. The harmonic intensity depends more sensitively on source separation. In the range of $500\,\text{eV} < \hbar\omega_X < 560\,\text{eV}$, the optimum source distance shifts from $d_{\text{max,500}} \approx 1.5$ mm to $d_{\text{max,560}} \approx 1.2$ mm with $d_{\text{FWHM}} < 0.5$ mm. Figure 4b and c show the dependence of the harmonic yield on $\hbar\omega_X$ and d for selected values of d and $\hbar\omega_X$, respectively.

DISCUSSION

At first sight, the observed optimum source distances of 1.3–1.7 mm seem to be far too large. The phase shift of the laser field induced by the Gouy effect between the two sources[34] separated to this extent shifts the phase of the atomic dipole oscillations by $\approx 10\pi$ at frequencies in the 400 eV range. The long rephasing length has a similar origin to the enhanced phase-matching reported above. Diffraction of the laser beam causes not only an advance of the phase of the laser field but also a decrease of its amplitude due to the divergence of the beam, which causes a comparable shift of the dipole phase of opposite sign in our experiment. Whereas a change of the laser phase by $\Delta\varphi_L$ shifts the phase of the qth harmonic by $q\Delta\varphi_L$, a change of the laser intensity by ΔI_L adds $\alpha\Delta I_L$ to the dipole phase with $\alpha \sim 10^{-13}\,\text{W}^{-1}\,\text{cm}^2$ (the exact value of α is sensitive to the choice of an electron trajectory)[35]. Hence, the positive phase shift induced by the Gouy effect can be partially compensated by a decrease of the laser intensity between the jets due to diffraction. A 10π decrease of the dipole phase would result from a change of the intensity of the divergent laser beam by $\Delta I_L \sim -3 \times 10^{14}\,\text{W}\,\text{cm}^{-2}$. This value seems to be close to the estimated decrease in on-axis peak intensity resulting from the beam divergence between the sources in our experiment.

The experimental data shown in Figs 3 and 4 clearly indicate that by varying the distance between the sources we can have the harmonic waves originating from the first and the second source destructively or constructively interfere. At high photon energies (in particular around 400 eV and above 500 eV) the contrast between constructive and destructive interference substantially exceeds an order of magnitude, providing conclusive evidence for the coherence of the SXR harmonic waves and the high quality of their coherent superposition. This contrast significantly decreases towards lower photon energies (below 300 eV). In addition, the sensitivity of the harmonic yield to the source distance is conspicuously lower for harmonics in the 200–400 eV range than for higher energies (>500 eV), as is obvious from Fig. 4a,c. We believe that this is due to the fact that lower-energy harmonics emerge over a broader temporal interval during the laser pulse, as well as from a larger spatial volume, experiencing thereby very different phase-matching conditions owing to differences in the (local) laser field parameters. Hence harmonics of the same order emerging from the two sources at different instants (in the local coordinate system of the laser pulse) may interfere constructively at different source separations. In contrast, high-energy harmonics are created in a smaller temporal window and spatial volume, implying more sharply defined phase-matching conditions, resulting in the more pronounced dependence of their yield on small changes in the source separation. This same reason is probably responsible for the vanishing modulation of harmonic yield at 330 eV for $p_b > 40$ mbar in Fig. 2.

The complex spatiotemporal dynamics of the coherent growth of high-order harmonics compromises the utility of conventional QPM schemes relying on periodic structures. After traversing through a few periods of the QPM structure, the electric-field waveform might suffer some small distortions. This leads to modified phase-matching conditions and calls for readjustment of the parameters (for example, the period) of the QPM structure for continued harmonic growth. Distortion of the laser field speeds up for shorter pulses. This is why QPM had not been successful in the few-cycle regime before. To benefit from QPM and the dramatic increase in the amplitude of high-frequency dipole oscillations when being driven with a few-cycle field[24], the QPM structure requires more degrees of freedom.

PROSPECTS

We believe that the experiments presented here open the prospect for combining the powerful concept of QPM with the power of few-cycle drivers for high-order harmonic generation. In fact, coherent addition of harmonics originating from different sources, as proposed and demonstrated here, offers—by individual adjustment of the source separation, density and the position of the beam waist within the structure—all the freedom necessary to adapt the system parameters to the changing conditions for optimum harmonic growth as the few-cycle driver propagates through the generation medium. Several challenges remain to be addressed with the most critical one being the defocusing of the laser beam by the radial variation of free-electron density as the beam propagates through an extended interaction medium comprising many separate sources. Using a driver beam with a near-rectangular-shaped (for example, super-gaussian) transverse profile constitutes one possible way of addressing this issue. Alternatively (or in addition), a longer-wavelength few-cycle driver[36,37] may alleviate this problem, owing to its ability to generate high-energy harmonics at a substantially reduced ionization level. Although several technical challenges remain to be solved, we believe that the presented route to the development of a powerful coherent kiloelectronvolt-scale source is most promising and justifies further efforts.

Received 24 May 2007; accepted 1 October 2007; published 11 November 2007.

References

1. Macklin, J. J., Kmetec, J. D. & Gordon III, C. L. High-order harmonic generation using intense femtosecond pulses. *Phys. Rev. Lett.* **70**, 766–769 (1993).
2. L'Huillier, A. & Balcou, Ph. High-order harmonic generation in rare gases with a 1-ps 1053-nm laser. *Phys. Rev. Lett.* **70**, 774–777 (1993).
3. Spielmann, Ch. *et al.* Generation of coherent X-rays in the water window using 5-femtosecond laser pulses. *Science* **278**, 661–664 (1997).
4. Constant, E. *et al.* Optimizing high harmonic generation in absorbing gases: Model and experiment. *Phys. Rev. Lett.* **82**, 1668–1671 (1999).
5. Schnürer, M. *et al.* Absorption-limited generation of coherent ultrashort soft-X-ray pulses. *Phys. Rev. Lett.* **83**, 722–725 (1999).
6. Takahashi, E., Nabekawa, Y. & Midorikawa, K. Generation of 10-μJ coherent extreme-ultraviolet light by use of high-order harmonics. *Opt. Lett.* **27**, 1920–1922 (2002).
7. Hergott, J.-F. *et al.* Extreme-ultraviolet high-order harmonic pulses in the microjoule range. *Phys. Rev. A* **66**, 021801(R) (2002).

8. Gibson, E. A. *et al.* Coherent soft X-ray generation in the water window with quasi-phase matching. *Science* **302**, 95–98 (2003).
9. Seres, E., Seres, J., Krausz, F. & Spielmann, Ch. Generation of coherent soft-X-ray radiation extending far beyond the titanium L edge. *Phys. Rev. Lett.* **92**, 163002 (2004).
10. Seres, J. *et al.* Source of coherent kiloelectronvolt X-rays. *Nature* **433**, 596 (2005).
11. Seres, E., Seres, J. & Spielmann, Ch. X-ray absorption spectroscopy in the keV range with laser generated high harmonic radiation. *Appl. Phys. Lett.* **89**, 181919 (2006).
12. Pfeifer, T., Spielmann, Ch. & Gerber, G. Femtosecond X-ray science. *Rep. Prog. Phys.* **69**, 443–505 (2006).
13. Kobayashi, Y., Sekikawa, T., Nabekawa, Y. & Watanabe, S. 27-fs extreme ultraviolet pulse generation by high-order harmonics. *Opt. Lett.* **23**, 64–66 (1998).
14. Tzallas, P., Charalambidis, D., Papadogiannis, N. A., Witte, K. & Tsakiris, G. Direct observation of attosecond light bunching. *Nature* **426**, 267–271 (2003).
15. Sekikawa, T., Kosuge, A., Kanai, T. & Watanabe, S. Nonlinear optics in the extreme ultraviolet. *Nature* **432**, 605–608 (2004).
16. Nikolopoulos, L. A. A. *et al.* Second-order autocorrelation of an XUV attosecond pulse train. *Phys. Rev. Lett.* **94**, 113905 (2005).
17. Nabekawa, Y. *et al.* Interferometric autocorrelation of an attosecond pulse train in the single-cycle regime. *Phys. Rev. Lett.* **97**, 153904 (2006).
18. Paul, P. M. *et al.* Observation of a train of attosecond pulses from high harmonic generation. *Science* **292**, 1689–1692 (2001).
19. Hentschel, M. *et al.* Attosecond metrology. *Nature* **414**, 509–513 (2001).
20. Drescher, M. *et al.* Time-resolved atomic inner-shell spectroscopy. *Nature* **419**, 803–807 (2002).
21. Uiberacker, M. *et al.* Attosecond real-time observation of electron tunnelling in atoms. *Nature* **466**, 627–632 (2007).
22. Agostini, P. & DiMauro, L. F. The physics of attosecond light pulses. *Rep. Prog. Phys.* **67**, 813–855 (2004).
23. Corkum, P. B. & Krausz, F. Attosecond science. *Nature Phys.* **3**, 381–387 (2007).
24. Brabec, T. & Krausz, F. Intense few-cycle laser fields: frontiers of nonlinear optics. *Rev. Mod. Phys.* **72**, 545–591 (2000).
25. Zhang, X. *et al.* Quasi-phase-matching and quantum-path control of high-harmonic generation using counterpropagating light. *Nature Phys.* **3**, 270–275 (2007).
26. Lytle, A. L. *et al.* Probe of high-order harmonic generation in a hollow waveguide geometry using counterpropagating light. *Phys. Rev. Lett.* **98**, 123904 (2007).
27. Geissler, M., Tempea, G. & Brabec, T. Phase-matched high-order harmonic generation in the non adiabatic limit. *Phys. Rev. A* **62**, 033817 (2000).
28. Paul, A. *et al.* Quasi-phase-matched generation of coherent extreme ultraviolet light. *Nature* **421**, 51–54 (2003).
29. Lompre, L. A. *et al.* High-order harmonic generation in xenon: intensity and propagation effects. *J. Opt. Soc. Am. B* **7**, 754–761 (1990).
30. Seres, J. *et al.* Sub-10-fs, terawatt-scale Ti:sapphire laser system. *Opt. Lett.* **28**, 1832–1834 (2003).
31. Hauri, C. P. *et al.* Generation of intense, carrier-envelope phase-locked few-cycle laser pulses through filamentation. *Appl. Phys. B* **79**, 673–677 (2004).
32. Seres, J. *et al.* Generation of coherent keV x-rays with intense femtosecond laser pulses. *New J. Phys.* **8**, 251 (2006).
33. Tempea, G., Geissler, M., Schnürer, M. & Brabec, T. Self-phase-matched high harmonic generation. *Phys. Rev. Lett.* **84**, 4329–4332 (2000).
34. Lindner, F. *et al.* Gouy phase shift for few-cycle laser pulses. *Phys. Rev. Lett.* **92**, 113001 (2004).
35. Balcou, P., Dederichs, A. S., Gaarde, M. B. & L'Huillier, A. Quantum-path analysis and phase matching of high-order harmonic generation and high-order frequency mixing processes in strong laser fields. *J. Phys. B* **32**, 2973–2989 (1999).
36. Fuji, T. *et al.* Parametric amplification of few-cycle carrier-envelope phase-stable pulses at 2.1 μm. *Opt. Lett.* **31**, 1103–1105 (2006).
37. Hauri, C. P. *et al.* Intense self-compressed, self-phase-stabilized few-cycle pulses at 2 μm from an optical filament. *Opt. Lett.* **32**, 868–870 (2007).

Acknowledgements

This study has been sponsored by the Austrian Science Fund (grant Nos F016 P02, P03 and Z63), the DFG grant SP 687/1-3 and the DFG Cluster of Excellence Munich Centre for Advanced Photonics—MAP (http://www.munich-photonics.de). We gratefully acknowledge gas-flow simulations by K. Schmid and friendly support from A. Baltuska.
Correspondence and requests for materials should be addressed to F.K.